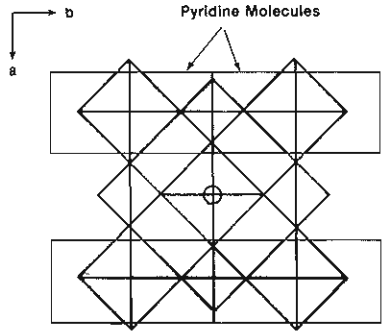

Figure 7. van der Waals area occupied by pyridine molecules coordinated to the surface of a single $VOPO_4$ layer, demonstrating the possibility of ligand interpenetration.

bonding model that has pyridine coordinated to vanadium with the ligand plane perpendicular to the layers. While it is difficult to predict exactly the *c* axes of these coordination intercalates without knowledge of the metal–ligand bond distance and the structural details of the oxide layer itself, it can be assumed that these factors remain constant as the ligand size increases. Thus, from CPK molecular models, the difference in van der Waals length along the coordination axis between pyridine and 4-phenylpyridine can be easily measured and compared directly to the observed *c*-axis differences. The 4.6-Å expansion observed on going from $VOPO_4$(py) to $VOPO_4$(4-Phpy) corresponds closely to the differences in length of the ligands (4.4 Å). This indicates that, in the $VOPO_4$ compounds, pyridine molecules from adjacent layers interpenetrate, since the total expansion is that caused by a single ligand. On the $VOPO_4$ layer surface, the coordination sites are 6.2 Å apart. This is only a little less than the van der Waals width of pyridine, 6.4 Å, allowing the ligands to line up along the *a* axis as shown in Figure 7 and stack in an interlocking fashion along the *c* axis.

The ligand-packing arrangement in $VOPO_4$(py) is different from that of the analogous MoO_3 compound,[4] which has coordination sites 5.3 Å apart. On the MoO_3 surface the pyridine molecules are more densely packed so no interpenetration of ligands from adjacent layers is possible. As a result the *c*-axis difference in MoO_3(py) and MoO_3(4-Phpy) is 8.8 Å, twice the difference in length of the ligands.

In summary, vanadyl phosphate and arsenate react with pyridine and 4-substituted pyridines to form coordination intercalation compounds. The pyridine molecules replace either a coordinated water molecule in $VOPO_4 \cdot 2H_2O$ or a vanadyl oxygen from an adjacent layer in the anhydrous hosts. In the compounds the pyridine molecules are perpendicular to the oxide layers and little or no reduction of the V^{5+} centers occurs. Reactions with 4-substituted pyridines are much slower than with pyridine itself, and the products are less crystalline than those formed with pyridine. These coordination intercalation compounds are analogous to those previously reported for MoO_3 and WO_3. We are currently extending this general type of reaction to other $MOXO_4$ host lattices.

Acknowledgment. We thank B. G. Silbernagel and L. A. Gebhard for measuring the ESR spectra.

Registry No. $VOPO_4 \cdot 2H_2O$, 12293-87-7; $VOPO_4 \cdot H_2O$, 61156-00-1; α-$VOPO_4$, 12395-27-2; $VOAsO_4 \cdot 2H_2O$, 12291-57-5; $VOPO_4$(py), 82648-60-0; $VOPO_4$(4,4'-bpy), 82648-61-1; $VOPO_4$(4-Phpy), 82648-62-2; $VOAsO_4$(py), 82648-63-3.

Contribution from the Department of Chemistry, Florida Atlantic University, Boca Raton, Florida 33431, and Contribution No. 756 from the Charles F. Kettering Research Laboratory, Yellow Springs, Ohio 45387

Eight-Coordinate Complexes of Molybdenum with 1,1-Dithio Ligands. Synthesis, Electrochemistry, and Spectroscopic Properties

DORIS A. SMITH,[1a] JOHN W. McDONALD,[1b] HARRY O. FINKLEA,[1a] VIRGINIA R. OTT,[1a] and FRANKLIN A. SCHULTZ*[1a]

Received February 5, 1982

Syntheses, characterization, and electrochemical and spectroscopic properties are reported for a series of eight-coordinate molybdenum(V) complexes with 1,1-disubstituted ethylenedithiolate ($Mo(S_2C_2R_2)_4^{3-}$; R = CN, COOEt), dithiocarbamate ($Mo(S_2CNEt_2)_4^+$), and thioxanthate ($Mo(S_2CS\text{-}t\text{-}Bu)_4^+$) ligands. The compounds each exhibit a reversible Mo(V) → Mo(VI) oxidation and a reversible Mo(V) → Mo(IV) reduction with the exception of $Mo(S_2CS\text{-}t\text{-}Bu)_4^+$, for which no oxidation is observed. The half-wave potentials of these reversible processes span a range of +1.2 to −1.7 V vs. SCE in CH_3CN and CH_2Cl_2. Irreversible oxidation of some of the Mo(VI) species and irreversible reduction of some of the Mo(IV) species also are observed. Thin-layer spectroelectrochemistry is used to obtain visible spectra of the oxidized and reduced complexes, establish the Nernstian character of the Mo(VI)/Mo(V) and Mo(V)/Mo(IV) redox couples, and investigate the catalytic behavior of the electrogenerated Mo(VI) species, $Mo(S_2CNEt_2)_4^{2+}$.

Introduction

The occurrence of Mo–S bonding in molybdenum-containing enzymes[2] has generated current interest in complexes of this metal with sulfur-containing ligands.[3] 1,1-Dithio ligands[4] form sulfur-rich complexes with most transition metals. Dithiocarbamates,[5-7] thioxanthates,[7] and dithiobenzoates[7-9] form tetrakis complexes with the higher oxidation states of molybdenum and thereby provide an eight-sulfur (MoS_8) coordination environment for this element.

In this paper we report the preparation and characterization of a new series of eight-coordinate molybdenum complexes with the dinegative ethylenedithiolate (ed) ligands 1,1-di-

(1) (a) Florida Atlantic University. (b) Charles F. Kettering Research Laboratory.
(2) (a) Newton, W. E., Otsuka, S., Eds. "Molybdenum Chemistry of Biological Significance"; Plenum Press: New York, 1980. (b) Coughlan, M. P., Ed. "Molybdenum and Molybdenum-Containing Enzymes"; Pergamon Press: Oxford, 1980.
(3) (a) Stiefel, E. I. *Prog. Inorg. Chem.* **1977**, *22*, 1. (b) Stiefel, E. I. In ref 2b, Chapter 2.
(4) (a) Coucouvanis, D. *Prog. Inorg. Chem.* **1970**, *11*, 233. (b) *Ibid.* **1979**, *26*, 301.
(5) Nieuwpoort, A. Ph.D. Thesis, University of Nijmegen, The Netherlands, 1975.
(6) (a) Nieuwpoort, A.; Steggerda, J. J. *Recl. Trav. Chim. Pays-Bas* **1976**, *95*, 250. (c) *Ibid.* **1976**, *95*, 289. (c) *Ibid.* **1976**, *95*, 294.
(7) Hyde, J.; Zubieta, J. *J. Inorg. Nucl. Chem.* **1977**, *39*, 289.
(8) Piovesana, O.; Sestili, L. *Inorg. Chem.* **1974**, *13*, 2745.
(9) Roberie, T.; Hoberman, A. E.; Selbin, J. *J. Coord. Chem.* **1979**, *9*, 79.

0020-1669/82/1321-3825$01.25/0

cyano-2,2-ethylenedithiolate (*i*-mnt) (**1a**), 1-cyano-1-carbethoxy-2,2-ethylenedithiolate (ced) (**1b**), and 1,1-dicarbethoxy-2,2-ethylenedithiolate (ded) (**1c**). The redox and spectroscopic properties of these complexes and of those previously reported with *N*,*N*-diethyldithiocarbamate (Et_2dtc)[5-7] (**2**) and *tert*-butyl thioxanthate (*t*-Butxn)[7] (**3**) ligands are examined by cyclic voltammetry, controlled-potential coulometry, thin-layer spectroelectrochemistry, and visible absorption and EPR spectroscopy. The results establish the range of electrochemical and spectroscopic behavior associated with the MoS_8 center and the extent to which these properties are influenced by the structure of the 1,1-dithio ligand.

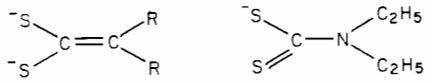

1a, $R_1 = R_2 = CN$
b, $R_1 = CN$, $R_2 = COOC_2H_5$
c, $R_1 = R_2 = COOC_2H_5$

2

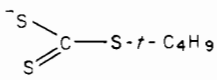

3

Experimental Section

Synthetic Procedures. The dipotassium salts of the three ethylenedithiolate ligands, K_2(*i*-mnt), K_2(ced), and K_2(ded), were prepared by known procedures.[10] Sodium *tert*-butyl thioxanthate, Na(*t*-Butxn), was prepared as described by Hyde and Zubieta.[7] Pyridinium oxopentachloromolybdate(V), $(pyH)_2MoOCl_5$, was prepared as described by Sasaki et al.[11] Other starting materials were obtained commercially and used without purification. All syntheses were carried out in a fume hood, and the products were stored under vacuum. Elemental analyses were performed by Galbraith Laboratories, Inc., Knoxville, TN.

(n-Bu_4N)$_3$Mo(*i*-mnt)$_4$. A solution of $(pyH)_2MoOCl_5$ (3.6 g, 8.0 mmol) in 50 mL of ethanol/water (1:1) was purged with nitrogen for 10 min to remove HCl. This solution was added to K_2(*i*-mnt) (7.0 g, 32.0 mmol) dissolved in 50 mL of ethanol/water (1:1). The resulting red-brown solution was refluxed for 90 min. The solution was allowed to cool to room temperature, and tetra-*n*-butylammonium bromide, n-Bu_4NBr (5.2 g, 16 mmol), was added. After overnight refrigeration, a green waxy solid precipitated and was isolated by filtration. This material was washed with 1:1 ethanol/water (4 × 25 mL), 4:1 ethanol/water (12 × 25 mL), and ethanol (4 × 25 mL) until the washings were no longer colored. Yield: 65%.

(n-Bu_4N)$_3$Mo(ced)$_4$. A solution of $(pyH)_2MoOCl_5$ (6.8 g, 15 mmol) in 100 mL of ethanol/acetonitrile (1:1) was added to a suspension of K_2(ced) (16.0 g, 60 mmol) in 100 mL of the same solvent. The mixture was refluxed for 90 min, allowed to cool to room temperature, and filtered. After addition of $(n\text{-}Bu)_4NBr$ (14.5 g, 45 mmol) to the filtrate, the mixture was filtered again. The solvent was allowed to evaporate from the filtrate, leaving a brown tar. Cyclic voltammetry of this material in CH_3CN solvent revealed the presence of several components. Attempts to isolate the desired Mo(ced)$_4^{3-}$ complex by recrystallization were unsuccessful. Purification was accomplished by column chromatography (5 cm × 12 cm) on alumina (Fisher A-540, 80–200 mesh) with dichloromethane/acetone mixtures as eluants. A broad, amber band eluted first with 2:1 CH_2Cl_2/acetone. The Mo(ced)$_4^{3-}$ complex eluted as a dark brown band with 1:2 CH_2Cl_2/acetone. The solvent was evaporated under a stream of dry nitrogen. Recrystallization of the product was not necessary. Yield: 8%.

(n-Pr_4N)$_3$Mo(ded)$_4$. This compound was prepared by the procedure given for (n-Bu_4N)$_3$Mo(ced)$_4$, except that the materials used were $(pyH)_2MoOCl_5$ (9.0 g, 20 mmol), K_2(ded) (25.0 g, 80 mmol), and tetra-*n*-propylammonium bromide, n-Pr_4NBr (16.0 g, 60 mmol). The dark brown product was purified by chromatography on alumina using CH_2Cl_2/acetone mixtures as eluants and recrystallized from acetone. Yield: 3%.

Mo(Et_2dtc)$_4$$PF_6$. Procedure A reported in ref 6a for the preparation of Mo(Et_2dtc)$_4$Br was followed until the point of product isolation. Potassium hexafluorophosphate (5.5 g, 30 mmol) was added to the solution (30 mmol of Mo(Et_2dtc)$_4$Br in 100 mL of diglyme), and the mixture was heated until all solids dissolved. The solution was cooled to room temperature, and the brown product in quantitative yield was collected by filtration and recrystallized three times from acetone.

Mo(*t*-Butxn)$_4$. A solution of $(pyH)_2MoOCl_5$ (4.5 g, 10 mmol) in 50 mL of water was deoxygenated with argon and added to a deoxygenated solution of Na(*t*-Butxn) (15.1 g, 80 mmol) in 20 mL of water at 2 °C. Concentrated hydrochloric acid was added dropwise until a dark solid precipitated. This material was collected by filtration under nitrogen and dried under vacuum. The complex was purified by chromatography on Florisil (Fisher F-101, 100–200 mesh) and recrystallized from carbon disulfide/pentane as described in ref 7. UV–visible spectra and cyclic voltammetric traces obtained for the blue product were in good agreement with published data.[7] Yield: 35%.

Mo(*t*-Butxn)$_4^+$. Solutions of this Mo(V)–thioxanthate complex were generated in two ways: (i) controlled-potential oxidation of Mo(*t*-Butxn)$_4$ at +0.7 V vs. SCE in 0.1 M n-Bu_4NPF_6/CH_2Cl_2 and (ii) oxidation of Mo(*t*-Butxn)$_4$ in CH_2Cl_2 by stoichiometric addition of a spectrophotometrically standardized[12] solution of Br_2 in CH_3CN. Cyclic voltammetric traces of the resulting red solutions confirmed complete oxidation to the Mo(V) state. We were unable to isolate a pure solid sample of the Mo(*t*-Butxn)$_4^+$ complex as had been reported previously for Mo(*i*-Prtxn)$_4$$PF_6$.[7]

(n-Pr_4N)$_2$$S_2C_2R_2$ (R = CN, $COOC_2H_5$). Tetra-*n*-propylammonium salts of the ethylenedithiolate ligands were prepared by adding the dipotassium salt of each ligand (10 mmol) to 20 mmol of n-Pr_4NBr in 20 mL of water. The product was extracted into an equal volume of dichloromethane, which was evaporated to yield (n-Pr_4N)$_2$(*i*-mnt) and (n-Pr_4N)$_2$(ced) as yellow solids and (n-Pr_4N)$_2$(ded) as a viscous yellow oil.

Instrumentation. Cyclic voltammetric experiments were conducted with a solid-state operational amplifier potentiostat constructed in this laboratory. Traces were recorded on a Hewlett-Packard Model 7035B X-Y recorder. Voltammetric experiments were conducted in a Brinkmann E615 cell using a Beckman 39273 Pt-button working electrode (area 0.20 cm^2), a Pt-wire auxiliary electrode, and a commercial aqueous saturated calomel reference electrode (SCE). The reference electrode was isolated from the test solution by a salt bridge containing supporting electrolyte and solvent. All potentials are reported vs. the aqueous SCE.

Controlled-potential coulometric experiments were conducted by use of an EG&G Princeton Applied Research (PAR) Model 173/179 potentiostat and digital coulometer. Current was measured during coulometry by use of a Fluke 8010A digital multimeter connected to the current output terminal of the 179. The working electrode for coulometry was a 12-cm^2 piece of Pt foil. The reference electrode was described above. The auxiliary electrode was a Pt coil separated from the sample solution by a 4–8-μm glass frit. Cells, glassware, supporting electrolyte, and the Pt electrodes were dried overnight at 100 °C before each electrochemical experiment. All solutions were deoxygenated and blanketed with dry nitrogen or argon that had passed through a solvent washing tower. All electrochemical experiments were carried out at ambient temperature (22 ± 2 °C).

Thin-layer electrochemistry and spectroelectrochemistry were accomplished by use of an optically transparent, thin-layer electrode (OTTLE) cell, which has been described previously[13] and is based on the design of Anderson et al.[14] In the present experiments the OTTLE cell incorporated a gold-minigrid (1.0 × 1.5 cm, 100 lines/in., Buckbee-Mears Co., St. Paul, MN) working electrode and a Pt-needle auxiliary electrode; a saturated calomel reference electrode was connected to the cell by a nonaqueous salt bridge. Deoxygenated sample solutions were transferred to the cell under pressure of inert gas through Teflon tubing.

In spectroelectrochemical experiments, visible absorption data at 350–700 nm were obtained as a function applied potential with the

(10) Jensen, K. A.; Henriksen, L. *Acta Chem. Scand.* **1968**, *22*, 1107.
(11) Sasaki, Y.; Taylor, R. S.; Sykes, A. G. *J. Chem. Soc., Dalton Trans.* **1975**, 396.
(12) Callahan, R. W.; Brown, G. M.; Meyer, T. J. *Inorg. Chem.* **1975**, *14*, 1443.
(13) Charney, L. M.; Finklea, H. O.; Schultz, F. A. *Inorg. Chem.* **1982**, *21*, 549.
(14) Anderson, C. W.; Halsall, H. B.; Heineman, W. R. *Anal. Biochem.* **1979**, *93*, 366.

Table I. Analytical, Conductivity, and Infrared and EPR Spectroscopic Data

complex	% found (% calcd) C	H	N	Mo	S
$Mo(Et_2dtc)_4PF_6$	28.66 (28.80)	4.75 (4.83)		11.43 (11.50)	
$(n\text{-}Bu_4N)_3Mo(i\text{-}mnt)_4$	55.35 (55.54)	7.97 (7.87)	10.98 (11.13)	6.83 (6.93)	18.43 (18.53)
$(n\text{-}Bu_4N)_3Mo(ced)_4$	54.78 (55.00)	8.20 (8.21)	6.14 (6.24)	6.29 (6.10)	16.12 (16.31)
$(n\text{-}Pr_4N)_3Mo(ded)_4$	51.46 (51.30)	7.95 (7.85)	2.68 (2.64)	5.83 (6.03)	15.98 (16.11)

complex	Λ_M,[a] $cm^2\ \Omega^{-1}\ mol^{-1}$	freq, cm^{-1} [c] Mo–S	$X{=}CS_2$ (X = N, C)	C=O	C≡N	g[d]	10^4A-(^{95,97}Mo), cm^{-1} [d]
$Mo(Et_2dtc)_4PF_6$	140	359 m	1505 s (1472 s)			1.980	34.1
$(n\text{-}Bu_4N)_3Mo(i\text{-}mnt)_4$	313	346 w	1385, 1405 s (1360 s)		2199 s (2174, 2199, 2225 s)	1.979	32.7
$(n\text{-}Bu_4N)_3Mo(ced)_4$	291	341 w	1394 s (1363 s)	1660 s (1654 s)	2187 s (2177, 2194 s)	1.982	32.0
$(n\text{-}Pr_4N)_3Mo(ded)_4$	363[b]	338 w	1374, 1397 s (1365 s)	1654 m (1658 m)		1.983	32.2

[a] At 10^{-3} M in CH_3CN. [b] 2.5×10^{-4} M. [c] Values in parentheses are for the $n\text{-}Pr_4N^+$ salts of the ligands. [d] In CH_2Cl_2 at room temperature. For $Mo(t\text{-}Butxn)_4^+$, $g = 1.981$ and $A = 30.4 \times 10^{-4}\ cm^{-1}$ were observed upon oxidation of $Mo(t\text{-}Butxn)_4$ in CH_2Cl_2 with Br_2.

OTTLE cell located in the sample compartment of a Harrick RSS-C rapid-scan spectrophotometer and attached to the PAR 173 potentiostat. Spectral data were digitized and processed by a Nova 2 minicomputer and were plotted on the Hewlett-Packard recorder. Cell thickness and cell volume were calibrated with solutions of potassium ferricyanide in water.

Electronic spectra from 350 to 900 nm also were recorded on a Cary 14 or Perkin-Elmer 575 spectrophotometer. The latter instrument was used to obtain charge-transfer spectra of the Mo(VI)–ed complexes since the absorptions were outside the range of the RSS-C. Dichloromethane solutions of $Mo(i\text{-}mnt)_4^{3-}$ and $Mo(ced)_4^{3-}$, oxidized with Br_2, and of $Mo(ded)_4^{3-}$, oxidized with I_2, were used for this purpose.

Room-temperature EPR spectra of dichloromethane solutions of the isolated Mo(V) complexes were recorded at 9.52 GHz by use of a Varian Model 4502 spectrometer. The EPR spectrum of $Mo(t\text{-}Butxn)_4^+$ was acquired after oxidizing a solution of $Mo(t\text{-}Butxn)_4$ in CH_2Cl_2 with Br_2.

Infrared spectra of the Mo(V) complexes and the $n\text{-}Pr_4N^+$ salts of the ligands were obtained on a Perkin-Elmer 621 spectrometer. Solid samples were run as KBr disks; $(n\text{-}Pr_4N)_2(ded)$ was run as a neat liquid between AgCl plates.

Conductance measurements were made with a Yellow Springs Instruments Model 31 conductivity bridge with aqueous solutions of KCl as standards.

Reagents. Spectrophotometric grade acetonitrile and dichloromethane (Aldrich) were stored over activated molecular sieves and used as electrochemical and spectroscopic solvents. The supporting electrolytes were tetraethylammonium tetrafluoroborate ($(TEA)BF_4$) and tetra-*n*-butylammonium hexafluorophosphate ($(TBA)PF_6$) from Southwestern Analytical Chemicals.

Results and Discussion

Preparation and Characterization. Analytical, conductivity, and infrared and EPR spectroscopic data (Table I), electrochemical data (Table II), and visible absorption data (Table III) indicate that the ed complexes are isolated as trinegative ions containing the Mo(V) oxidation state. Preparation of these complexes demonstrates that the ethylenedithiolates parallel other 1,1-dithio ligands in their ability to form eight-coordinate complexes with early transition elements.[4,15] Particularly notable is the capacity of these ligands to stabilize non-oxo molybdenum in its highest formal oxidation states. As suggested by the redox potentials in Table II, isolation of non-oxo $Mo^{VI}S_8$ species should be possible with ed ligands.

Previous syntheses of MoS_8 complexes have utilized oxidative decarbonylation of $Mo(CO)_6$ or $Mo(CO)_5X^-$ ($X = Cl^-$, Br^-, I^-) by the disulfide form of the ligand[5-7] as well as ligand displacement from oxo[7,16] and non-oxo[8,9] complexes of molybdenum. Not having the oxidized forms of the ligands in hand, we chose to prepare the ed complexes by ligand displacement from readily synthesized[11] $(pyH)_2MoOCl_5$. This approach is effective in the preparation of $Mo(i\text{-}mnt)_4^{3-}$, where the oxo group is readily cleaved from Mo(V), even in the presence of H_2O, and the desired complex is isolated in good yield. Preparation of the ced and ded complexes by this route proved to be more difficult. Ligand displacement provided these complexes in low yield, and chromatographic separation from mixtures with unidentified side products was required. Improved synthetic procedures are being sought for the ced and ded complexes.

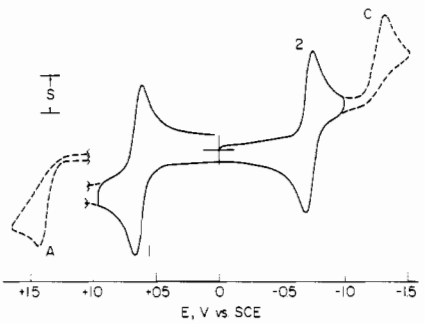

Figure 1. Cyclic voltammogram of 0.23 mM $(n\text{-}Bu_4N)_3Mo(i\text{-}mnt)_4$ in CH_3CN (0.1 M $(TEA)BF_4$); $v = 0.2\ V\ s^{-1}$. $S = 50\ \mu A\ cm^{-2}$ for waves 1, 2, and C; $S = 200\ \mu A\ cm^{-2}$ for wave A.

In the infrared spectrum (Table I) the frequency of the $C{=}CS_2$ vibration is seen to increase by 25–45 cm^{-1} upon coordination of the ed dianion. This increment is similar to the shift of ca. 35 cm^{-1} in $\nu(N{=}CS_2)$ upon coordination of Et_2dtc^- as $Mo(Et_2dtc)_4^+$. Our values for $\nu(C{=}CS_2)$ are consistent with strong bands observed at ~1400 cm^{-1} in $Ni(i\text{-}mnt)_2^{2-}$, $Cu(i\text{-}mnt)_2^{2-}$, and $Fe(i\text{-}mnt)_3^{3-}$[17] but differ significantly from a recent tabulation[18] that assigns $\nu(C{=}CS_2)$ at ≥1450 cm^{-1} for analogous ded complexes.

Cyclic Voltammetry and Controlled-Potential Coulometry. Electrochemical behavior of the MoS_8 complexes is represented by the cyclic voltammogram of $Mo(i\text{-}mnt)_4^{3-}$ shown in Figure 1. Starting in the Mo(V) oxidation state, we observed one reversible oxidation (wave 1) and one reversible reduction (wave 2) for this compound. Waves 1 and 2 occur for all five

(15) Willemse, J.; Cras, J. A.; Steggerda, J. J.; Keijzers, C. P. *Struct. Bonding (Berlin)* **1976**, *28*, 83.

(16) McAuliffe, C. A.; Sayle, B. J. *Inorg. Chim. Acta* **1975**, *12*, L7.
(17) Fackler, J. P., Jr.; Coucouvanis, D. *J. Am. Chem. Soc.* **1966**, *88*, 3913.
(18) Reference 4b, Table XXVI.

Table II. Electrochemical Data[a]

complex	wave A E_p, V[b]	wave A $i_p/v^{1/2}AC$[d]	wave A n[e]	wave 1 $E_{1/2}$, V[c]	wave 1 $i_p/v^{1/2}AC$[d]	wave 1 n[e]
			Acetonitrile (0.2 M (TEA)BF_4)			
Mo(*t*-Butxn)$_4^+$						
Mo(Et$_2$dtc)$_4^+$				+1.153 (68)	950	0.95
Mo(*i*-mnt)$_4^{3-}$	+1.433 (73)	3162	4	+0.654 (66)	828	1.02
Mo(ced)$_4^{3-}$	+1.208 (78)	2788	4	+0.304 (64)	812	1.00
Mo(ded)$_4^{3-}$	+0.800 (45)	1665	2	−0.132 (62)	705	1.02
			Dichloromethane (0.1 M (TBA)PF_6)			
Mo(*t*-Butxn)$_4^+$						
Mo(Et$_2$dtc)$_4^+$				+1.129 (113)	885	1
Mo(*i*-mnt)$_4^{3-}$	+1.510 (71)	1768	2	+0.519 (85)	870	1
Mo(ced)$_4^{3-}$	+1.060 (74)	1571	2	+0.175 (113)	730	1
Mo(ded)$_4^{3-}$	+0.830 (56)	1650	2	−0.302 (101)	710	1

complex	wave 2 $E_{1/2}$, V[c]	wave 2 $i_p/v^{1/2}AC$[d]	wave 2 n[e]	wave C E_p, V[b]	wave C $i_p/v^{1/2}AC$[d]	wave C n[e]
			Acetonitrile (0.2 M (TEA)BF_4)			
Mo(*t*-Butxn)$_4^+$	+0.494 (63)	*f*	*f*	−0.730 (82)	*f*	*f*
Mo(Et$_2$dtc)$_4^+$	−0.444 (66)	965	1	−1.141 (66)	969	1
Mo(*i*-mnt)$_4^{3-}$	−0.715 (64)	888	1	−1.295 (65)	767	1
Mo(ced)$_4^{3-}$	−1.024 (63)	800	1			
Mo(ded)$_4^{3-}$	−1.472 (67)	773	1			
			Dichloromethane (0.1 M (TBA)PF_6)			
Mo(*t*-Butxn)$_4^+$	+0.369 (78)	985	0.99	−0.953 (87)	1673	2
Mo(Et$_2$dtc)$_4^+$	−0.550 (105)	915	1	−1.283 (122)	811	1
Mo(*i*-mnt)$_4^{3-}$	−0.843 (84)	740	1	−1.723 (123)	566	1
Mo(ced)$_4^{3-}$	−1.178 (144)	850	1			
Mo(ded)$_4^{3-}$	−1.672 (139)	1060[g]	1			

[a] 0.2–1 mM complexes; data for waves 1 and 2 averaged over v = 0.01–0.2 V s^{-1}; data for waves A and C at v = 0.1 V s^{-1}. [b] Irreversible peak potential; number in parentheses is $|E_p - E_p/2|$ in mV. [c] Reversible half-wave potential = $(E_{pa} + E_{pc})/2$; number in parentheses is ΔE_p in mV. [d] Units of A s$^{1/2}$ cm V$^{-1/2}$ mol^{-1}. [e] Number of electrons determined by controlled-potential coulometry or comparison of voltammetric peak current parameters (see text). [f] Concentration of complex unknown due to low solubility. [g] $i_p/v^{1/2}AC$ increases and i_{pr}/i_{pf} decreases as v decreases.

Table III. Electronic Spectral Data[a]

complex	λ_{max}, nm (ϵ, M^{-1} cm^{-1})
Mo(*t*-Butxn)$_4^+$[b]	424 sh (8800), 480 (6610), 524 (6200), 561 (6030), 604 sh (4800)
Mo(*t*-Butxn)$_4$[b]	472 sh (3040), 513 (3900), 633 (5250)
Mo(Et$_2$dtc)$_4^{2+}$	459 (2020), 670 (11 200)
Mo(Et$_2$dtc)$_4^+$	397 (5360), 450 (5510), 460 (5580), 492 sh (2820), 525 (1890)
Mo(Et$_2$dtc)$_4$	400 sh (2100), 448 sh (2000), 480 (2440), 515 (2290), 567 (1770)
Mo(*i*-mnt)$_4^{2-}$	475 sh (4300), 860 (9830)[c]
Mo(*i*-mnt)$_4^{3-}$	408 sh (12 800), 464 (14 800), 572 (9450), 628 sh (3040), 672 (3320)
Mo(*i*-mnt)$_4^{4-}$	418 sh (11 400), 452 (12 400), 528 (5250), 638 (2620)
Mo(ced)$_4^{2-}$	450 sh (6650), 823 (13 700)[c]
Mo(ced)$_4^{3-}$	412 sh (16 400), 467 (15 200), 554 (9900), 634 (3920)
Mo(ced)$_4^{4-}$	558 (6450), 656 (7380)
Mo(ded)$_4^{2-}$	455 sh (6300), 792 (10 700)[d]
Mo(ded)$_4^{3-}$	463 (15 500), 545 (8340), 638 (3490)
Mo(ded)$_4^{4-}$	580 (4500), >680 sh (4800)

[a] In CH_3CN (0.2 M (TEA)BF_4). [b] In CH_2Cl_2 (0.2 M (TBA)PF_6). [c] Recorded in CH_2Cl_2 after oxidation of Mo(V) complex with Br_2. [d] Recorded in CH_2Cl_2 after oxidation of Mo(V) complex with I_2.

complexes with the exception of Mo(*t*-Butxn)$_4^+$, for which no oxidation is observed. At more positive potentials an irreversible oxidation (wave A) occurs also in the case of the *i*-mnt, ced, and ded complexes, and at more negative potentials an irreversible reduction (wave C), in the case of the *i*-mnt, Et$_2$dtc, and *t*-Butxn complexes. Electrochemical data for these redox processes in CH_3CN and CH_2Cl_2 solvents are summarized in Table II.

Waves 1 and 2 are judged to be reversible, diffusion-controlled, one-electron transfers on the basis of the cyclic voltammetric data. Values of $i_p/v^{1/2}AC$ are constant to within ±5%, and i_{pr}/i_{pf} = 1.00 ± 0.05 over the range v = 0.01–0.2 V s^{-1} for waves 1 and 2 in both solvents. The only exception to this behavior occurs in the case of Mo(ded)$_4^{3-}$ in CH_2Cl_2, for which wave 2 lies close to the background discharge of the solvent. The peak potential separations (ΔE_p) in CH_3CN range from 62 to 68 mV, which is close to the expected value for a reversible one-electron transfer.[19] The larger values of ΔE_p observed in CH_2Cl_2 are attributed in part to the larger amount of uncompensated solution resistance in this solvent.

The number of electrons transferred in wave 1 for the ded, ced, *i*-mnt, and Et$_2$dtc complexes and in wave 2 for the *t*-Butxn complex was confirmed by controlled-potential coulometry. Coulometric oxidation of Mo(ded)$_4^{3-}$ (at +0.10 V), Mo(ced)$_4^{3-}$ (+0.50 V), and Mo(*i*-mnt)$_4^{3-}$ (+0.85 V) in CH_3CN produced currents that decayed smoothly to background levels and provided linear log i vs. t plots. Values of n = 1.02, 1.00, and 1.02, respectively, were obtained from the coulometric data. Oxidation of Mo(Et$_2$dtc)$_4^+$ at +1.30 V in CH_3CN resulted after 45 min in a steady-state current which was ca. one-third of the initial current. Treatment of the data as described previously[20,21] for a catalytic chemical reaction in controlled-potential coulometry gave n = 0.95. Apparently, the oxidation product of Mo(Et$_2$dtc)$_4^+$ reacts catalytically with the solvent medium on the time scale of bulk-solution coulometry, although the oxidation of Mo(Et$_2$dtc)$_4^+$ is reversible and dif-

(19) Nicholson, R. S. *Anal. Chem.* **1965**, *37*, 1351.
(20) Ott, V. R.; Schultz, F. A. *J. Electroanal. Chem. Interfacial Electrochem.* **1975**, *61*, 81.
(21) Bard, A. J.; Faulkner, L. R. "Electrochemical Methods. Fundamentals and Applications"; Wiley: New York, 1980; pp 476–477.

fusion controlled on the shorter time scale of cyclic voltammetry. Coulometric oxidation of Mo(*t*-Butxn)$_4$ was accomplished at +0.6 V in CH_2Cl_2. Current was almost constant initially but decayed smoothly to the background level after 30 min. A value of $n = 0.99$ was calculated from the total coulombs passed in the experiment.

Values of n for the other redox steps were estimated by comparing voltammetric peak current parameters. A value of $n = 1$ was assigned to the remaining reversible electron transfers, because $(i_p/v^{1/2}AC)_1$ and $(i_p/v^{1/2}AC)_2$ have nearly the same magnitudes for all complexes in a given solvent. For the irreversible processes, n was estimated by comparing peak current parameters of waves A and C to those of the corresponding reversible reactions by using relationship 1,[22] where

$$n_{irrev} = \frac{0.90(i_p/v^{1/2}AC)_{irrev}}{(i_p/v^{1/2}AC)_{rev}} \frac{n^{3/2}_{rev}}{(\alpha n_a)^{1/2}_{irrev}} \quad (1)$$

$\alpha n_a = 0.0477/(E_p - E_{p/2})$ (in V). The electron stoichiometries determined in this manner for waves 1, 2, A, and C are listed in Table II.

The electrochemical behavior of the MoS_8 complexes is described by the series of reactions (2)–(5). Reactions 3 and

$$Mo^{VI}S_8 - ne^- \rightarrow \text{products} \quad (E_p)_A \quad (2)$$

$$Mo^{VI}S_8 + e^- \rightleftharpoons Mo^{V}S_8 \quad (E_{1/2})_1 \quad (3)$$

$$Mo^{V}S_8 + e^- \rightleftharpoons Mo^{IV}S_8 \quad (E_{1/2})_2 \quad (4)$$

$$Mo^{IV}S_8 + ne^- \rightarrow \text{products} \quad (E_p)_C \quad (5)$$

4 (waves 1 and 2) are assigned to reversible, metal-centered electron transfers, which constitute Mo(VI)/Mo(V) and Mo(V)/Mo(IV) redox couples. Reactions 2 and 5 (waves A and C) are assigned to oxidations above or reductions below these levels. These steps are irreversible and result in the transfer of either single or multiple electrons, which may imply substantial ligand character to the redox orbital.

The notable electrochemical feature of the MoS_8 complexes is the large sensitivity of the metal-centered redox processes to changes in ligand structure; indeed, the reversible half-wave potentials in Table II exhibit a total range of nearly 3 V. The shifts in $E_{1/2}$ are consistent with the expectation that electron-withdrawing substituents favor reduction and electron-donating substituents favor oxidation of the metal center. In a separate paper[23] we present a detailed interpretation of the shifts in $E_{1/2}$ and their correlation with ligand substituent parameters, molecular structural features, and spectroscopic properties of the MoS_8 complexes. The ability to predictably adjust reversible, metal-centered redox potentials over such a wide range suggests possible useful applications for these compounds as electron-transfer mediators or homogeneous catalysts.

Electronic Spectra. Visible absorption data for stable oxidation levels of all five MoS_8 complexes are reported in Table III. Except where noted, these spectral results were obtained under potentiostatic control in the OTTLE cell. The experimentally demonstrated reversibility of the redox conversions under these conditions confirms the spectroscopic features assigned to the various oxidation states. Our spectral results agree well with previous reports for Mo(Et$_2$dtc)$_4^+$,[6b,24] Mo(Et$_2$dtc)$_4$,[6c] and Mo(*t*-Butxn)$_4$,[7] but we note some differences between our results and those reported in $CHCl_3$ for Mo(*t*-Butxn)$_4^+$.[7] Some uncertainty is associated with the spectral parameters reported for Mo(Et$_2$dtc)$_4^{2+}$, because of the catalytic

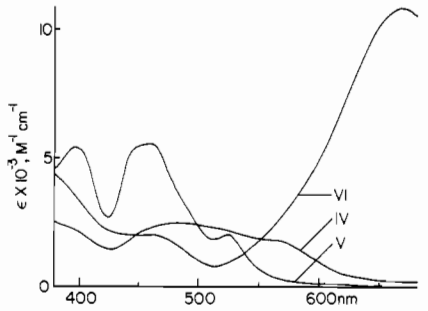

Figure 2. Visible absorption spectra of Mo(Et$_2$dtc)$_4^{2+,+,0}$ species in CH_3CN (0.2 M (TEA)BF_4) obtained under constant potential conditions in the OTTLE cell. Potentials used to generate the oxidation states: Mo(VI), +1.4 V; Mo(V), 0.0 V; Mo(IV), −0.7 V.

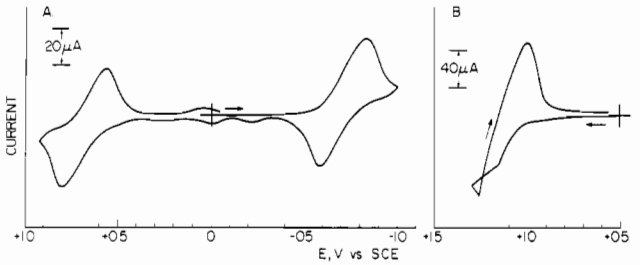

Figure 3. Thin-layer cyclic voltammograms in the OTTLE cell of (A) 1.21 mM (n-Bu$_4$N)$_3$Mo(i-mnt)$_4$ and (B) 1.95 mM Mo(Et$_2$dtc)$_4$PF$_6$. v = 4 mV s^{-1}, and the solvent is CH_3CN (0.2 M (TEA)BF_4).

reaction of this species with the solvent medium. However, conversion to the Mo(VI) oxidation state must be nearly quantitative under the conditions of thin-layer electrolysis because spectral features characteristic of Mo(V) are absent from the Mo(Et$_2$dtc)$_4^{2+}$ spectrum. Spectra of the Mo(Et$_2$dtc)$_4^{2+,+,0}$ oxidation states obtained in the OTTLE cell are shown in Figure 2.

The prominent spectral feature of the Mo(VI) complexes is a single intense absorption at 670–860 nm, which is assignable to ligand-to-metal charge transfer on the basis of the d^0 configuration of the metal. The molybdenum(V)–ethylenedithiolate complexes exhibit a distinctive pattern of charge-transfer absorptions, observable as a progression of three bands at 463–467, 545–572, and 643–672 nm (see Figure 4 for an example). Similar, but less perfectly ordered, absorptions are observed for the Mo(Et$_2$dtc)$_4^+$ and Mo(*t*-Butxn)$_4^+$ species. The Mo(IV) complex Mo(i-mnt)$_4^{4-}$ also displays a series of three charge-transfer bands, but this feature is absent from the spectra of Mo(ced)$_4^{4-}$ and Mo(ded)$_4^{4-}$. Absorption bands for the Mo(ed)$_4^{2-}$ and Mo(ed)$_4^{3-}$ complexes shift to lower energy as their redox potentials become more positive (stronger electron-withdrawing substituents). This trend is consistent with L → M charge transfer. However, the effect of ligand structure on these spectral properties (Table III) is small in comparison to the effect on redox potentials (Table II).

Thin-Layer Electrochemistry and Spectroelectrochemistry. The technique of spectroelectrochemistry in thin layers of solution[25] has been applied increasingly to the study of inorganic redox systems.[13,26] Benefits of this methodology include

(22) Adams, R. N. "Electrochemistry at Solid Electrodes"; Marcel Dekker: New York, 1969; pp 115–139.
(23) Smith, D. A.; Schultz, F. A. *Inorg. Chem.* **1982**, *21*, 3035.
(24) Garner, C. D.; Howlader, N. C.; Mabbs, F. E.; McPhail, A. T.; Miller, R. W.; Onan, K. D. *J. Chem. Soc., Dalton Trans.* **1978**, 1582.
(25) (a) Kuwana, T.; Heineman, W. R. *Acc. Chem. Res.* **1976**, *9*, 241. (b) Heineman, W. R. *Anal. Chem.* **1978**, *50*, 390A. (c) DeAngelis, T. P.; Heineman, W. R. *J. Chem. Educ.* **1976**, *53*, 594.
(26) (a) Rohrbach, D. F.; Deutsch, E.; Heineman, W. R.; Pasternack, R. F. *Inorg. Chem.* **1977**, *16*, 2650. (b) Rohrbach, D. F.; Deutsch, E.; Heineman, W. R. In "Characterization of Solutes in Nonaqueous Solvents"; Mamantov, G., Ed.; Plenum Press: New York, 1978; pp 177–195. (c) Rohrbach, D. F.; Heineman, W. R.; Deutsch, E. *Inorg. Chem.* **1979**, *18*, 2536.

Table IV. Thin-Layer Electrochemical and Spectroelectrochemical Data[a]

complex	process	$2.3RT/nF$,[b] mV	n[b]	$E^{\circ\prime}_{SE}$,[b] V	$E^{\circ\prime}_{TL}$,[c] V	$E_{1/2}$,[d] V
$Mo(i\text{-mnt})_4^{3-}$	V → VI	63.2 ± 1.1	0.94	+0.680 ± 0.001	+0.680 (237)	+0.654
	V → IV	65.2 ± 2.5	0.91	−0.719 ± 0.002	−0.715 (248)	−0.715
$Mo(ced)_4^{3-}$	V → VI	61.1 ± 1.3	0.97	+0.318 ± 0.001	+0.327 (210)	+0.304
	V → IV	58.1 ± 2.0	1.02	−1.034 ± 0.003	−1.035 (230)	−1.024
$Mo(ded)_4^{3-}$	V → VI	59.9 ± 2.7	0.99	−0.124 ± 0.003	−0.125 (140)	−0.132
	V → IV	61.5 ± 2.3	0.96	−1.493 ± 0.001	−1.505 (172)	−1.472

[a] In CH_3CN (0.2 M $(TEA)BF_4$), with 0.4–1.0 mM complex, at 24 ± 2 °C; results were averaged over four data sets. [b] Determined by application of eq 6 using a monitoring wavelength of 464 nm. [c] Average of E_{pc} and E_{pa} from thin-layer cyclic voltammetry at $v = 4$ mV s^{-1}; ΔE_p in mV is shown in parentheses. [d] Half-wave potential determined by bulk-solution cyclic voltammetry at Pt electrode; from Table II.

the abilities to (i) derive additional information from the electrochemical part of the thin-layer experiment,[27] (ii) generate and obtain spectroscopic information about potentially reactive species within a period of a few minutes, and (iii) determine the formal potential ($E^{\circ\prime}_{SE}$) and electron stoichiometry (n) of a redox couple from simultaneous spectroscopic and electrochemical measurements by use of the Nernst equation.[25,26] We have used these approaches to further characterize the reversible electron-transfer steps of the MoS_8 complexes and to obtain the spectral information reported in Table III.

The thin-layer cyclic voltammogram in Figure 3A shows the reversible Mo(VI)/Mo(V) and Mo(V)/Mo(IV) redox couples of the $Mo(i\text{-mnt})_4^{3-}$ complex in CH_3CN. On the time scale of this experiment a small amount of electrode product decomposition is indicated by the presence of extraneous anodic peaks at −0.2 and 0.0 V following Mo(IV) generation and a cathodic peak at +0.05 V following Mo(VI) generation. Spectroscopic monitoring of the Mo(V) state indicates ~3–5% decomposition upon each cyclic Mo(V)/Mo(IV) or Mo(V)/Mo(VI) conversion. A similar amount of decomposition is noted following one-electron reduction of $Mo(ded)_4^{3-}$ in CH_3CN, but no decomposition is detectable in the case of the $Mo(ced)_4^{2-/3-}$, $Mo(ced)_4^{3-/4-}$, and $Mo(ded)_4^{2-/3-}$ couples in CH_3CN or the $Mo(t\text{-Butxn})_4^{+/0}$ couple in CH_2Cl_2.

Thin-layer cyclic voltammetric oxidation of $Mo(Et_2dtc)_4^+$ in CH_3CN produces an atypical current plateau at potentials more positive than +1.15 V as shown in Figure 3B. This result is attributed to catalytic oxidation of solvent or solvent impurities by the Mo(VI) electrode product, as observed also in the coulometric oxidation of $Mo(Et_2dtc)_4^+$ in bulk solution. After the electrode potential was returned in to 0 V the OTTLE experiment, spectroscopic measurements showed that $Mo(Et_2dtc)_4^+$ is regenerated with ≥85% efficiency. Thus, loss of material is less than would be expected if the Mo(VI) complex were to be irreversibly consumed during its chemical reaction. This result suggests possible application of $Mo(Et_2dtc)_4^{2+}$ and other highly oxidized MoS_8 species an oxidative redox catalysts.

Formal potentials and n values were determined for the ethylenedithiolate complexes in CH_3CN by means of spectropotentiostatic experiments in the OTTLE cell and the following form of the Nernst equation:[25,26]

$$E_{applied} = E^{\circ\prime}_{SE} + \frac{2.3RT}{nF} \log \frac{[O]}{[R]} \qquad (6)$$

The ratio [O]/[R] was determined spectrophotometrically at several applied potentials as the quantity $(A - A_R)/(A_O - A)$, where A is the absorbance measured for a mixture of O and R and A_O and A_R are the absorbances of the fully oxidized and fully reduced species. These quantities were corrected in appropriate cases for the small amounts of product decomposition noted above. A spectropotentiostatic experiment monitoring Mo(V) → Mo(VI) oxidation and Mo(V) → Mo(IV) reduction for $Mo(ced)_4^{3-}$ is illustrated in Figure 4. A clearly defined isosbestic point is observed in each case, as expected for the reversible conversion of one species to another. Values of $E^{\circ\prime}_{SE}$ and n determined from the intercept and slope of eq 6 are presented in Table IV. The results further substantiate the reversible, one-electron character of the Mo(VI)/Mo(V) and Mo(V)/Mo(IV) couples for the ethylenedithiolate complexes.

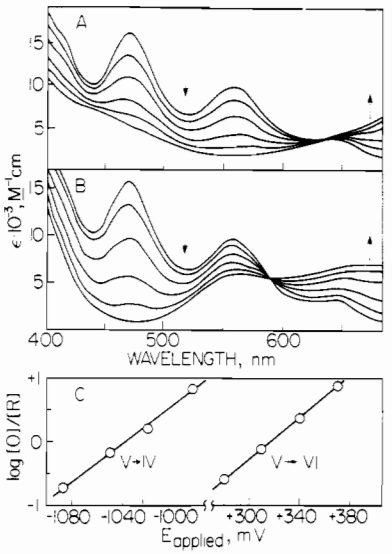

Figure 4. Spectropotentiostatic experiments for 0.94 mM $(n\text{-}Bu_4N)_3Mo(ced)_4$ in CH_3CN (0.2 M $(TBA)PF_6$): (A) spectra recorded during oxidation at 0, +0.280, +0.310, +0.340, +0.370, and +0.600 V; (B) spectra recorded during reduction at 0, −0.990, −1.020, −1.050, −1.080, and −1.350 V; (C) Nernst plots for Mo(V) → Mo(VI) and Mo(V) → Mo(IV) redox processes monitored at 464 nm.

Table IV also contains formal potentials determined simultaneously by thin-layer cyclic voltammetry ($E^{\circ\prime}_{TL}$). Agreement between the spectroelectrochemically and voltammetrically determined $E^{\circ\prime}$'s at the Au minigrid in the OTTLE cell is excellent. Agreement between these formal potentials and half-wave potentials determined by bulk-solution cyclic voltammetry at a Pt electrode ($E_{1/2}$, Table IV) also is good, but small systematic differences exist between $E^{\circ\prime}_{SE}$ or $E^{\circ\prime}_{TL}$ and $E_{1/2}$ ($E^{\circ\prime}_{SE} = 1.021\ E_{1/2} + 0.010$ V, $r = 0.9999$). The cause of this small discrepancy has not been identified.

Acknowledgment. Support of this research by the National Science Foundation under Grant CHE 80-20442 is gratefully acknowledged.

Registry No. $(n\text{-}Bu_4N)_3Mo(i\text{-mnt})_4$, 81643-67-6; $(n\text{-}Bu_4N)_3Mo(ced)_4$, 81642-88-8; $(n\text{-}Pr_4N)_3Mo(ded)_4$, 81642-90-2; $Mo(Et_2dtc)_4PF_6$, 81655-19-8; $Mo(t\text{-Butxn})_4$, 63576-35-2; $Mo(t\text{-Butxn})_4^+$, 82614-50-4; $Mo(Et_2dtc)_4^{2+}$, 82614-51-5; $Mo(Et_2dtc)_4$, 41947-30-2; $Mo(i\text{-mnt})_4^{2-}$, 81643-64-3; $Mo(i\text{-mnt})_4^{4-}$, 81643-61-0; $Mo(ced)_4^{2-}$, 81643-65-4; $Mo(ced)_4^{4-}$, 81643-62-1; $Mo(ded)_4^{2-}$, 81643-63-2; $Mo(ded)_4^{4-}$, 82614-52-6.

(27) Hubbard, A. T. *CRC Crit. Rev. Anal. Chem.* **1973**, *3*, 201.